MINERALOGICAL JOURNAL, VOL. 9, NO. 6, PP. 349-373, APRIL 1979

Polytypism of xonotlite: (I) Structure of an $A\bar{1}$ polytype

YASUHIRO KUDOH and YOSHIO TAKÉUCHI

Mineralogical Institute, Faculty of Science,
University of Tokyo, Hongo, Tokyo 113

ABSTRACT

Crystals of xonotlite from Heguri, Chiba Prefecture, Japan, which exhibit relatively sharp k odd reflections have been found to be a triclinic variant having dimensions; a 8.712(2) Å, b 7.363(2) Å, c 14.023(4) Å, $\alpha=89.99(2)°$, $\beta=90.36(2)°$, $\gamma=102.18(2)°$, and space group $A\bar{1}$; $Z=2[Ca_6Si_6O_{17}(OH)_2]$. The average structure which was determined using only even order reflections in k is similar to the reported average structure. Crystal-chemical consideration permitted to deconvolute the average structure to give the atomic arrangements for the true $A\bar{1}$ structure which has been refined to $R=4.0\%$ for observed reflections including odd order reflections in k. The structure consists of Si_6O_{17} double chains, each consisting of a pair of Si_3O_9 chains of the wollastonite type and sheets of polyhedra about Ca's. The structural scheme built up of these silicate chains and polyhedral sheets is similar to that of wollastonite though two of the three independent Ca atoms per cell are in trigonal prisms formed by oxygen atoms. Occupancy refinement of Ca appears to show that slight deficiency in Ca occurs only one of the three independent Ca sites.

The xonotlite polytypism can be discussed based on a monoclinic subcell, a_p 8.516Å, b_p 7.363Å, c_p 7.012Å, $\beta_p=90.37°$, underlying the $A\bar{1}$ structure. The polytypism may occur, unlike commonly known polytypism, in two directions, c and a: the monoclinic cell may be juxtaposed on (001) either in a continuous position or with a glide $b/2$, and on (100) with a glide $b/4$ (or $-b/4$).

Introduction

Xonotlite is a fibrous hydrated silicate of calcium whose chemical composition, $Ca_6Si_6O_{17}(OH)_2$, is closely related to that of wollastonite, $CaSiO_3$. Upon dehydration, xonotlite is in fact transformed into

wollastonite, the b-axis of which being parallel to the fibre axis, b, of xonotlite (Heller, 1951; Dent and Taylor, 1956).

Like wollastonite, xonotlite has a strong pseudo-translation of $\boldsymbol{b}/2$, reflections with k odd being very weak and tend to be badly drawn out thus hindering straightforward determination of its true crystal structure. Using k even reflections only, Mamedov and Belov (1955) carried out structural study and proposed the structure of a $P2/a$ xonotlite which contains double silicate chains each having the composition, $[Si_6O_{17}]^{10-}$. Although Gard (1966) reported, by electron-diffraction study, several polytypic variants of xonotlite crystals, it has since been unsuccessful to establish, by X-rays, any structure type of xonotlite. Further structural study is therefore of substantial need to elucidate full details of the structure, thereby providing a basis to discuss polytypism of this mineral species. The polytypism of xonotlite is of particular interest because its polytypic variants may occur in such a way that they vary both a and c periodicities, whereas those of wollastonite only the periodicity of a. In the following we give an account of the results of our study on xonotlite which has been carried out with the use of crystals exhibiting relatively sharp k odd reflections.

Experimental

Crystals used in the present investigation came from Heguri, Chiba Prefecture, Japan. The result of a wet chemical analysis (Table 1) is in good agreement with the ideal chemical formula of xonotlite, $Ca_6Si_6O_{17}(OH)_2$.

The crystals from this locality have a characteristics that they exhibit relatively sharp odd-level reflections about b though overlapped with diffuse streaks; thus they permitted us to determine the true crystal lattice of the material. Since the crystals have the shape of a fine needle, with b parallel to the needle, we recorded the reciprocal

Table 1. Chemical composition.

	Chemical analysis (Tiba, 1974)	Number of cations for 18 oxygen atoms
SiO_2	49.99 wt.%	5.986
Fe_2O_3	0.48	0.043
MnO	0.16	0.016
CaO	46.19	5.926
Na_2O	0.17	0.039
K_2O	0.02	0.003
$H_2O(+)$	2.95	2.356
$H_2O(-)$	0.10	
Total	100.06	

lattice with precession photographs about c and with de Jong-Bouman photographs about b. The recorded weak k odd reflections showed in the photographs an arrangement which simulates a monoclinic diffraction symmetry (Fig. 1). A closer examination into the photographs, however, revealed that so far the weak reflections are concerned their intensity distribution was not consistent with the (010) mirror plane characteristic of the monoclinic symmetry. This situation was readily interpreted that crystals were twinned, with (100) as composition plane, and twofold operation about b as twin operation; the twin individuals are triclinic, each having an A-centered cell (Fig. 2). The dimensions of the triclinic cell were determined based on a set of 15 reflections with k even only, which were recorded on a four-circle diffractometer (λ=0.70926Å); for the calculation to refine cell dimensions, was used the Appleman's program (Evans *et al.*, 1963). The cell dimensions thus obtained are given in Table 2. The unit cell contains two formula units, $Ca_6Si_6O_{17}(OH)_2$, giving a calculated density of 2.711 g·cm^{-3}. The centrosymmetric space group, $A1$, was confirmed through the subsequent

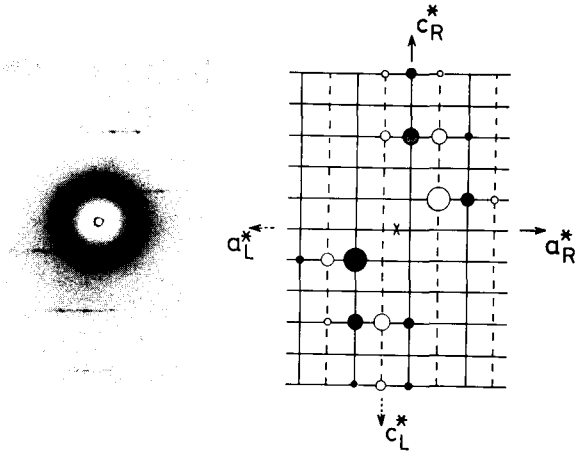

Fig. 1. Portion of the 1st-level de Jong-Bouman photograph of a twinned xonotlite crystal, showing sharp *h*1*l* reflections each accompanied by diffuse streaks along *a**. The diagram in the right gives the corresponding composite reciprocal net; weighted points from the twin individuals, denoted by R and L, are respectively indicated by solid and open circles.

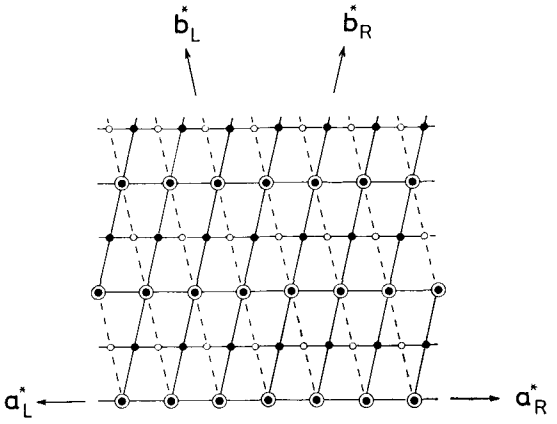

Fig. 2. Twinned reciprocal lattice of xonotlite, showing *hk*0 reciprocal nets of twin individuals R and L; reciprocal points are respectively indicated by solid and open circles. Note the composite reciprocal points that occur at the levels of *k* even.

Table 2. Comparison of crystallographic data for xonotlite.

	Pseudo-cell			True-cell*
	1	2	3	
a	16.53Å	17.029(1)Å	17.031(4)Å	8.712(2)Å
b	3.66	3.676(0)	3.682(1)	7.363(2)
c	7.04	7.005(1)	7.012(2)	14.023(4)
α	90°	90°	90°	89.99(2)°
β	90°	90.33(2)°	90.37(2)°	90.36(2)°
γ	90°	90°	90°	102.18(2)°
Space group	$C2/m$	$C2/m$	$C2/m$	$A\bar{1}$
Z	1	1	1	2

1. Mamedov and Belov (1955).
2. Xonotlite from Army Street, San Francisco, California (Kalousek *et al.*, 1977).
3. Xonotlite from Heguri, Chiba, Japan (this work).

* The $A\bar{1}$ cell of the Heguri specimen (this work).

structure analysis.

Although the crystals, which we so far examined, were unexceptionally twinned, the composite reflections with k even were, regardless the difference in volume ratio of twin individuals, consistent with a monoclinic symmetry, $C2/m$. This fact suggests that the distribution of k even reflections will have a monoclinic symmetry due to the existence of local mirror planes like the wollastonite case (Ito, 1950). This monoclinic cell, with b halved, is related to the true triclinic cell in the following way:

$$\begin{pmatrix} a_m \\ b_m \\ c_m \end{pmatrix} = \begin{pmatrix} 2 & 1/2 & 0 \\ 0 & 1/2 & 0 \\ 0 & 0 & 1/2 \end{pmatrix} \begin{pmatrix} a \\ b \\ c \end{pmatrix}$$

where a_m, b_m, c_m are the axes of the monoclinic cell and a, b, c those of the true cell. When the b axis of this monoclinic cell and is doubled,

the resulting cell has a symmetry which is consistent with $P2/a$ (Fig. 3). The dimensions of these cells are compared in Table 2.

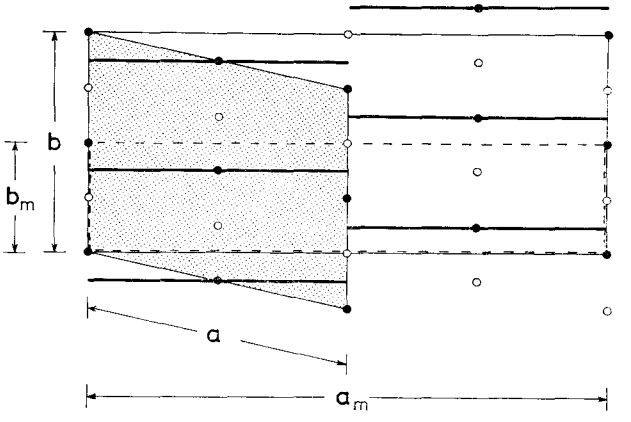

Fig. 3. The relationship between the A-centered triclinic cell (shaded) and the monoclinic pseudocell with b halved (broken lines); the Mamedov-Belov's $P2/a$ cell is indicated by light lines. For the triclinic cell, the inversion centers at the levels, $z=0$ and 1/2, are indicated by small solid circles, and those at the levels, $z=1/4$ and 3/4, by open circles.

For intensity collection, a twinned crystal was used which had approximate dimensions of $0.06\times0.25\times0.03\,mm^3$. The intensities of 1110 independent reflections with k even were recorded up to $\sin\theta/\lambda=0.70$ on a four-circle automatic diffractometer using graphite monochromated MoKα radiation. In this region of reciprocal space, we recorded 270 odd order reflections in k. After corrections for Lorentz and polarization factors, the intensities were reduced to structure factors. No corrections were made for absorption ($\mu=22.49\,cm^{-1}$) and extinction effect.

The reflections with k even correspond to the reflections from the average structure having the monoclinic cell, a_m, b_m, c_m, which is common to both individuals; each reflection is a composite of two

reflections which may be assumed to have, to a very close approximation, the same intensity because of the local mirrors (*vide infra*). Whereas the reflections with k odd, which we measured, are from only one of the twin individuals. We therefore used for structure refinement, different scale factors for these two different sets of reflections. We shall come to discuss this point later.

Determination of the structure

Average structure

The structure analysis was initiated with the determination of the monoclinic average structures having the unit cell a_m, b_m, c_m, and space group $C2/m$. As a starting model, the atomic coordinates were derived from those of the Mamedov-Belov's structure by superimposing the translation, $\boldsymbol{b}/2$, onto the structure. Regarding their structure, we should note that they assumed β angle to be 90°, which we measured as 90.37°. If one fails to detect, for β angle, such a small deviation from 90°, it is in general certainly impossible to distinguish one from the other of the two distinct sets of monoclinic axes, a, b, c and a', b', c' $(=a, b, \bar{c})$, giving rise to a possibility that $hk\bar{l}$ reflections, for example, are incorrectly assigned as hkl for a given set of axes. A comparison of the intensity distribution we obtained and that by Mamedov and Belov (1956) did reveal that their $hk\bar{l}$ reflections should be read as hkl for the conventional set of monoclinic axes with obtuse β angle. We therefore calculated structure factors after due transformation of the following form of the Mamedov-Belov's atomic coordinates:

$$\begin{pmatrix} x' \\ y' \\ z' \end{pmatrix} = \begin{pmatrix} -1 & 0 & 0 \\ 0 & -2 & 0 \\ 0 & 0 & 1 \end{pmatrix} \begin{pmatrix} x'' \\ y'' \\ z'' \end{pmatrix} + \begin{pmatrix} -1/4 \\ -1/4 \\ 0 \end{pmatrix}$$

where, x'', y'', z'' and x', y', z' are respectively the Mamedov-Belov's coordinates and the new ones.

The result of the initial structure-factor calculation gave the value of $R=0.133$. The monoclinic average structure was then refined by least-squares using the program LINUS (Coppens and Hamilton, 1970). For the calculations, nonionized atomic scattering factors were used which were taken from International Tables for X-ray Crystallography (1962). An anisotropic refinement using a weighting scheme, $w=1/(\sigma F_o)^2$, converged to give an $R=0.030$ for all observed even order reflections in k.

Deconvolution of the average structure

The atomic coordinates x', y', z' and thermal parameters β'_{ij} of the average structure can be transformed into those referred to the triclinic axes respectively by the following transformations:

$$\begin{pmatrix} x \\ y \\ z \end{pmatrix} = \boldsymbol{R} \begin{pmatrix} x' \\ y' \\ z' \end{pmatrix} + \begin{pmatrix} 1/2 \\ \pm 1/4 \\ -1/4 \end{pmatrix}$$

and

$$\begin{pmatrix} \beta_{11}, \beta_{12}, \beta_{13} \\ \beta_{12}, \beta_{22}, \beta_{23} \\ \beta_{13}, \beta_{23}, \beta_{33} \end{pmatrix} = \boldsymbol{R} \begin{pmatrix} \beta'_{11}, \beta'_{12}, \beta'_{13} \\ \beta'_{12}, \beta'_{22}, \beta'_{23} \\ \beta'_{13}, \beta'_{23}, \beta'_{33} \end{pmatrix} \tilde{\boldsymbol{R}},$$

where

$$\boldsymbol{R} = \begin{pmatrix} 2 & 0 & 0 \\ 1/2 & 1/2 & 0 \\ 0 & 0 & 1/2 \end{pmatrix}.$$

The set of atoms thus derived for the $A\bar{1}$ cell naturally bears exact translation of $\boldsymbol{b}/2$. Since however the average structure has very low R value and there is, in the difference Fourier map, essentially no residual peaks which suggest additional atomic locations or significant displacements from the atomic positions, crystal-chemical considerations readily permitted us to derive the true triclinic

structure from the above atomic set. The structure derived consists of silicate chains, $[Si_6O_{17}]^{10-}$ and bands of polyhedra about calcium atoms. Although the silicate chain has no longer pseudotranslation of $\boldsymbol{b}/2$, the polyhedral bands do have the pseudotranslation. This structural model was then refined using all observed reflections which include odd order reflections in k. Compared to the intensities of k even reflections, those of k odd reflections are less accurate owing to the overlappings of diffuse streaks along a^*. We therefore carefully examined those reflections recorded in X-ray films and omitted obviously unreliable sixteen reflections out of 270 reflections measured. A total of 1364 (=254+1110) reflections were then used for structure refinement.

The least-squares refinement which was executed in a way similar to that for the average-structure case converged to give $R=4.0\%$ for the whole set of reflections; 3.0% for k even reflections and 21% for k odd. Finally, we made an attempt of refining occupancy factors at the calcium sites. This was because xonotlite tends to be Ca-deficient (Grimmer and Wieker, 1971) though the effect is very small for the natural specimens (Kalousek *et al.*, 1977). Our specimen is indeed very slightly deficient in Ca although if Mn and monovalent cations such as Na and K are distributed at the Ca sites, the total cation number amounts to 5.984 for six available sites (Table 1). The result of the refinement which was carried out using scattering factor for Ca was: 0.990(3), 0.999(3) and 0.977(4) respectively at Ca(1), Ca(2) and Ca(3) sites. The deficiency at Ca(3) would seem to be significant; vacancies or monovalent cations, like Na, would perhaps be located around this site. The atomic coordinates and thermal parameters are respectively given in Table 3. A list of observed and calculated structure factors may be obtained upon request from the Mineralogical Institute of the University of Tokyo.

Table 3. Final atomic parameters for $A\bar{1}$ xonotlite.

Positional parameters				
Atom	x	y	z	B (Å^2)
Ca(1)	0.5046(4)	0.0016(5)	0.2523(3)	0.59
Ca(2)	0.1335(1)	0.1645(2)	0.1684(1)	0.84
Ca(3)	0.1385(1)	0.6537(1)	0.1707(1)	0.59
Si(1)	0.2118(2)	0.2170(2)	0.8841(1)	0.52
Si(2)	0.2118(1)	0.6389(2)	0.8843(1)	0.52
Si(3)	0.3182(1)	0.9547(2)	0.0281(1)	0.49
O(1)	1/2	0	0	1.65
O(2)	0.2190(4)	0.4303(5)	0.9211(2)	1.21
O(3)	0.3512(4)	0.7179(5)	0.8096(2)	0.97
O(4)	0.3434(4)	0.2059(5)	0.8087(2)	0.96
O(5)	0.2297(4)	0.1116(5)	0.9860(2)	1.00
O(6)	0.2294(4)	0.7538(5)	0.9858(2)	1.07
O(7)	0.0424(4)	0.6382(5)	0.8326(2)	0.92
O(8)	0.0463(4)	0.1339(5)	0.8370(2)	0.94
O(9)	0.2988(4)	0.9506(5)	0.1390(2)	0.49
O(10) (=OH)	0.2977(4)	0.4481(5)	0.1347(3)	1.32

Anisotropic temperature factors ($\times 10^4$)						
Atom	β_{11}	β_{22}	β_{33}	β_{12}	β_{13}	β_{23}
Ca(1)	13(1)	25(1)	11(0)	2(1)	−3(0)	−1(1)
Ca(2)	28(1)	30(2)	14(0)	11(1)	3(1)	5(1)
Ca(3)	20(1)	22(2)	10(0)	7(1)	0(1)	1(1)
Si(1)	22(2)	15(2)	8(1)	4(2)	0(1)	4(1)
Si(2)	19(2)	17(2)	8(1)	5(2)	0(1)	0(1)
Si(3)	13(2)	21(2)	8(1)	3(2)	1(1)	−1(1)
O(1)	32(7)	90(12)	27(3)	8(8)	6(4)	−3(5)
O(2)	61(6)	42(7)	14(2)	20(5)	−3(2)	−1(3)
O(3)	32(5)	41(7)	14(2)	9(5)	7(2)	0(3)
O(4)	32(5)	39(7)	14(2)	2(5)	0(2)	4(3)
O(5)	41(5)	48(7)	12(2)	21(5)	0(2)	4(3)
O(6)	45(5)	47(7)	11(2)	3(5)	2(2)	−4(3)
O(7)	15(4)	40(7)	19(2)	7(5)	−13(2)	−2(3)
O(8)	31(5)	56(7)	9(2)	2(5)	7(2)	4(3)
O(9)	28(4)	24(6)	2(1)	2(4)	−4(2)	1(2)
O(10) (=OH)	25(5)	69(8)	23(2)	10(5)	−2(2)	−3(3)

The evaluation of final atomic parameters

From the final atomic coordinates we calculated the deviation of each atomic pair from the local-mirror symmetry (Table 4). Although the average deviation is larger than that of wollastonite (Ito *et al.*, 1969; Yamanaka *et al.*, 1977), the deviations of most of the pairs are in the order of standard errors except the following three pairs: Ca(2), Ca(3); O(3), O(4); O(7), O(8); the mean deviation for these three pairs being 0.06Å. Because of such deviations from local mirror symmetry, the pair reflections for each composite reflections with k even in fact have not exactly the same intensity. A comparison of the observed sets of pair intensities however has revealed that the differences are less than $2\sigma(F^2)$. Therefore the major source of errors in the final atomic parameters is in the measured intensities of the

Table 4. Deviations of atom pairs from local mirror symmetry.

Atom pair	distance*
Ca(1)-Ca(1′)	0.003(3) Å
Ca(2)-Ca(3)	0.053(3)
Si(1)-Si(2)	0.003(2)
Si(3)-Si(3′)	0.002(2)
O(2)-O(2′)	0.004(5)
O(3)-O(4)	0.068(5)
O(5)-O(6)	0.006(5)
O(7)-O(8)	0.070(5)
O(9)-O(9′)	0.007(5)
O(10)-O(10′)	0.010(5)
mean	0.023

* The distance between one of the pair atoms, which are approximately related to each other by a local mirror plane, and the true image of the other due to the mirror operation.

odd-order reflections in k rather than the assumption that the sets of pair intensities have each identical values.

Discussion

General features of the structure

The structure of the triclinic variant of xonotlite is in principle similar to that of the monoclinic structure as proposed by Mamedov and Belov (1956). Among three independent Ca's per cell, Ca(1) is octahedrally surrounded by six oxygen atoms. The octahedra share edges, like those in wollastonite (Prewitt and Buerger, 1963), to form infinite chain along b. In contrast to the octahedral coordination about Ca(1), each of the other calcium atoms, Ca(2) and Ca(3), is coordinated by six oxygen atoms in the form of a trigonal prism with prismatical edges parallel to a plane perpendicular to b. Each of these calcium atoms has an additional oxygen atom respectively at a distance of 2.750Å (Ca(2)-O(5)) and 2.769Å (Ca(3)-O(6)), thus making the coordination in fact sevenfold. The polyhedra about Ca(2) and Ca(3), likewise, form, sharing edges, an infinite chain along b. These two kinds of chains are joined together, by sharing edges, to form a continuous sheet parallel to (001) (Fig. 4). The sheet and adjacent similar ones are joined together by silicate chains to form bulk of the structure (Fig. 5). The silicate chains, having a composition of Si_6O_{17}, consists of two Si_3O_9 chains, each of which is of the wollastonite type.

To show the relationship between the present structure and the structure given by Mamedov and Belov (1955), it is convenient to look upon the $A\bar{1}$ structure as a juxtaposition of certain monoclinic cells. Noting the existence of the monoclinic average structure, we can readily visualize such a monoclinic cell underlying the $A\bar{1}$ cell (Fig. 6). As will be observed in Fig. 6 the cell will have the following dimensions: a_p=8.516, b_p=7.363, c_p=7.012, β_p=90.37°. By analogy

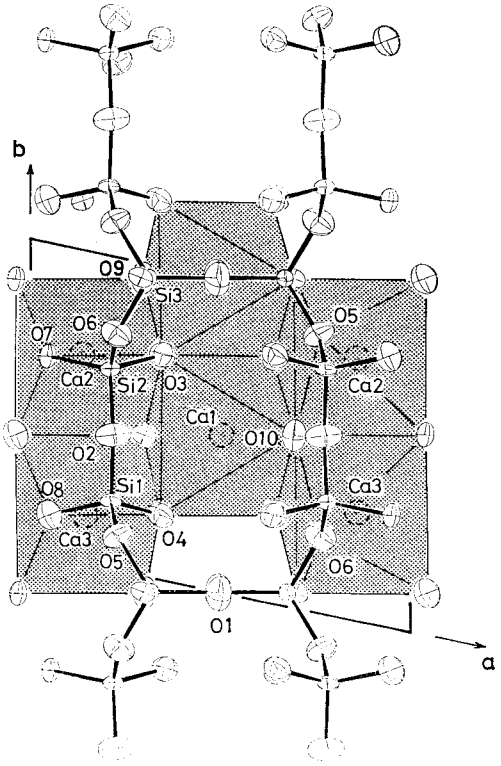

Fig. 4. The projection, onto (001), of the xonotlite structure in the slab bounded at $-0.33 \leqq z \leqq 0.20$. The thermal ellipsoids are drawn with the program ORTEP (Johnson, 1965). The Si-O bonds are shown by heavy lines.

of the wollastonite case (Ito, 1950), the hypothetical structure based on this cell will be called 'protoxonotlite' or *p*-xonotlite. In the $A\bar{1}$ structure, the cells of *p*-xonotlite are so juxtaposed on (100) with a glide $b/4$ (or $-b/4$) that the gliding occurs stepwise in the direction of a (Fig. 7a), and on (001) with glide $b/2$ that the gliding occurs alternately in the c-direction (Fig. 8b). Note that, in general, the

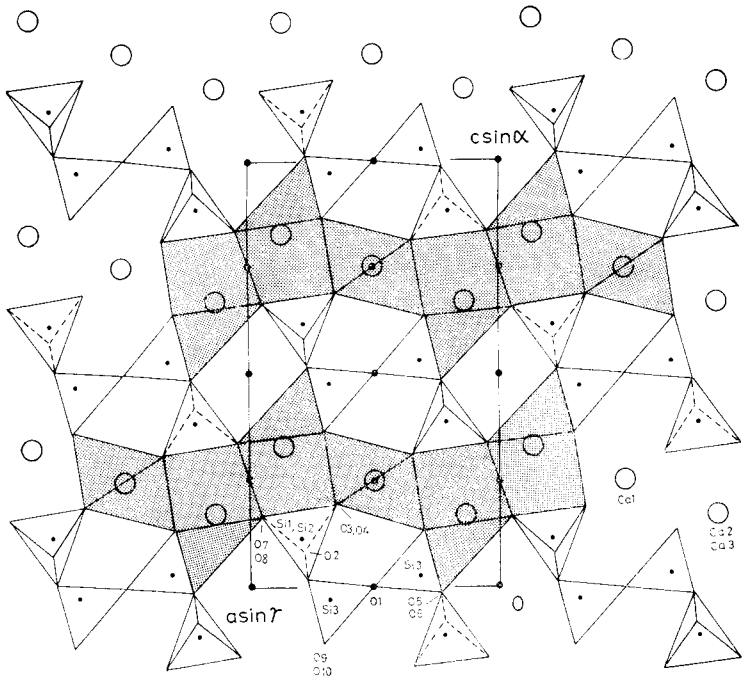

Fig. 5. The structure of xonotlite projected down the b axis, showing continuous sheets parallel to (001) (shaded) of Ca polyhedra. Large open circles represent calcium atoms.

juxtaposition of cells on (001) does not necessarily require the gliding of $b/2$; the cells may be placed in a continuous position. While, juxtapositions of cells on (100) necessarily require a gliding $b/4$ (or $-b/4$) to form crystal-chemically acceptable structure. The Mamedov-Belov's structure corresponds to the case in which the above gliding of $b/4$ (or $-b/4$) occurs not stepwise but alternately in the direction of a so that every other cells remain in position (Fig. 7b), and the glidings of cells, by $b/2$, do not occur in the direction of c (Fig. 8a). Polytypic variants of xonotlite structure can be derived based on these modes in relative arrangement of one to another cells of

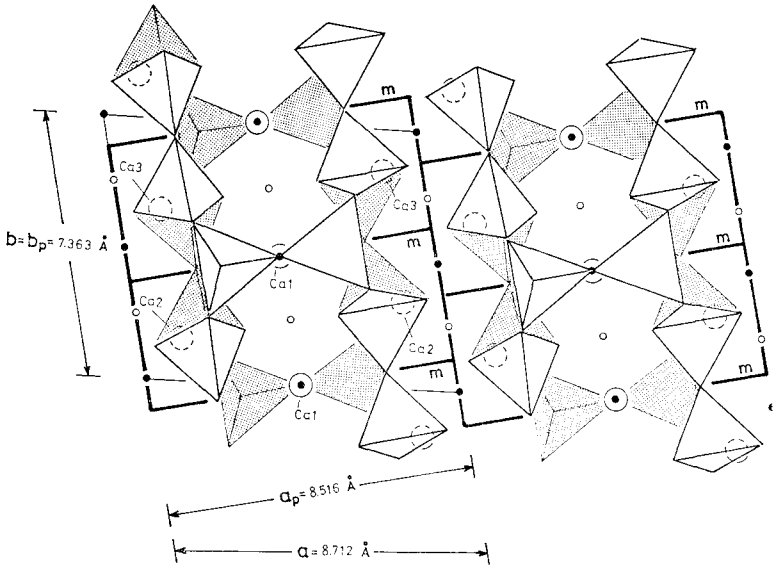

Fig. 6. The projection, onto (001), of the xonotlite structure in the slab bounded at $-0.17 \leqq z \leqq 0.70$. Heavy lines trace the cells of p-xonotlite, and light lines the triclinic cell; a_p and b_p denote the axes of the p-xonotlite cell, and m local mirror planes. The relative arrangement of silicate chains along c corresponds to that of the $A\bar{1}$ structure. Inversion centers are indicated as in Fig. 3.

p-xonotlite. An account will be given elsewhere of systematic derivation of xonotlite polytypes. We give in Table 5 the bond lengths of the $A\bar{1}$ xonotlite, and in Table 6 bond angles and interatomic distances.

The configuration of silicate chain

The pair of wollastonite chains that form a xonotlite silicate chain are linked together by sharing apical oxygen atoms locating at centers of symmetry (Fig. 4).

The double chain provides a rare example of the angle, 180°, that occurs at the set of bridge oxygen atoms, O(1). The isotropic tem-

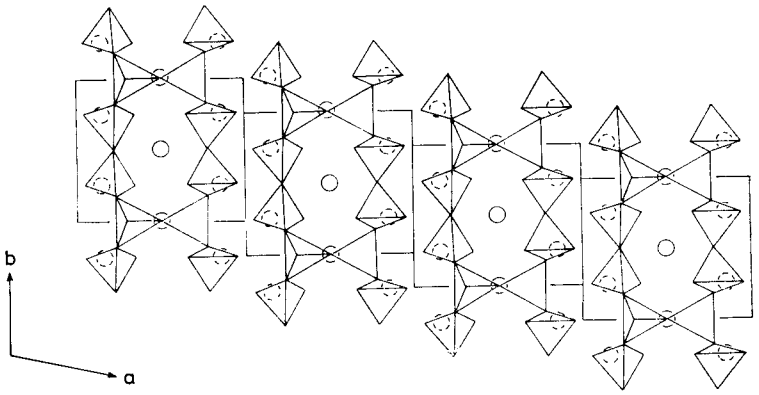

(a)

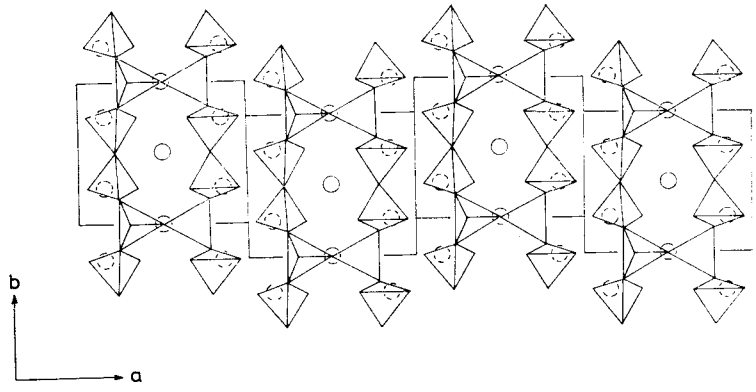

(b)

Fig. 7. Two stacking modes of *p*-xonotlite cells in the direction of the *a* axis: (a) stepwise gliding of $-b/4$, (b) alternate glidings of $b/4$ and $-b/4$. Light lines trace the unit cells of *p*-xonotlite.

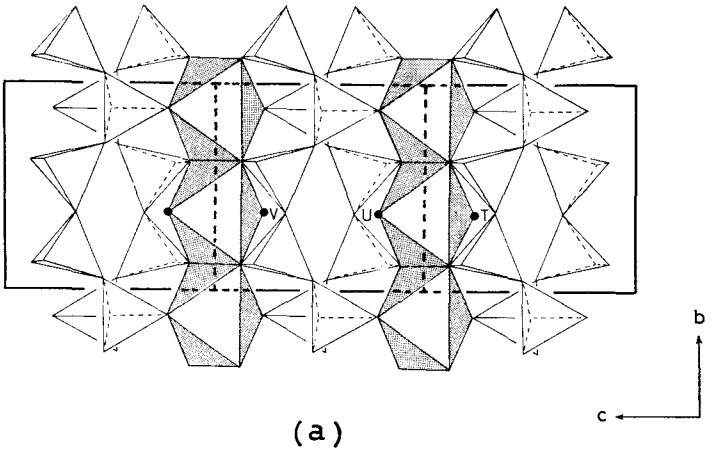

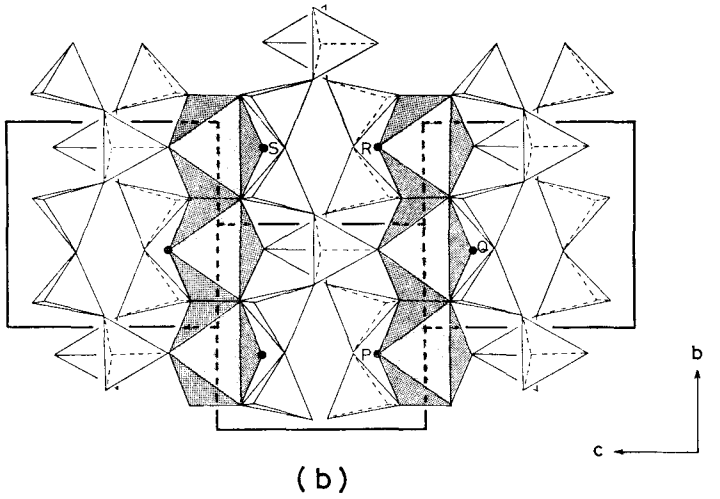

Fig. 8. Two stacking modes of *p*-xonotlite cells along *c*: (a) every cell is in parallel and continuous position, (b) every cell is displaced with respect to adjacent similar ones by *b*/2. In order to show the difference in the relative arrangement of OH groups due to the difference in stacking mode, a pair of octahedral columns of Ca is indicated in each figure, solid circles labelled P, Q, R, S, T and U representing OH groups. The OH-OH distances are P-Q=5.956Å, Q-R=5.991Å, R-S =U-V=5.128Å, T-U=4.710Å.

Table 5. Bond lengths and anionic valence sums (v. u.) for $A\bar{1}$ xonotlite.*

	Ca(1)	Ca(2)	Ca(3)	Si(1)	Si(2)	Si(3)	Σ
O(1)						1.600 1.01×2	2.02
O(2)				1.643 0.94	1.633 1.00		1.94
O(3)	2.348 0.35 2.425 0.32	2.704 0.20			1.621 1.03		1.90
O(4)	2.385 0.33 2.462 0.30		2.598 0.24	1.579 1.07			1.94
O(5)		2.750 0.18		1.649 0.93		1.627 0.96	2.07
O(6)			2.769 0.18		1.646 0.98	1.628 0.96	2.12
O(7)		2.323 0.35 2.435 0.30	2.383 0.32		1.639 0.99		1.96
O(8)		2.415 0.31	2.466 0.29 2.472 0.29	1.582 1.07			1.96
O(9)	2.358 0.34	2.386 0.32	2.376 0.33			1.565 1.08	2.07
O(10) (=OH)	2.305 0.36	2.319 0.35	2.316 0.36				1.07
Average	2.380	2.476	2.483	1.613	1.635	1.605	

* Computed with the valence sum program provided by Prof. Gabrielle Donnay (Donnay and Allmann, 1970).
The first line of each pair gives the bond length and the second the bond valence.

perature factor of O(1) shows a relatively large value (Table 3). The thermal ellipsoid of this oxygen atom however has features which are comparable with those of other bridge oxygen atoms such as O(2), O(5) and O(6) (Fig. 4). In addition, there appears to be no

Table 6. Edge lengths of polyhedra and bond angles.

Neighbours		Edge length	Angle
Octahedron about Ca(1)pq			
O(3)	O(3)q	3.046Å	79.3°
	O(4)	3.757	100.5
	O(9)pr	3.069	79.8
	O(10)p	3.607	99.3
O(3)q	O(4)r	3.608	99.3
	O(9)pr	3.551	98.0
	O(10)p	3.070	82.6
O(4)	O(4)r	3.144	80.9
	O(9)pr	3.058	78.7
	O(10)p	3.675	100.8
O(4)r	O(9)pr	3.615	99.3
	O(10)p	3.064	81.6
average		3.355	
Distorted octahedron about Ca(2)pq			
O(3)	O(7)	2.652Å	61.9°
	O(9)pr	3.069	73.9
	O(10)pq	3.070	74.9
O(5)rp	O(7)t	4.171	110.4
	O(8)s	3.668	90.3
	O(9)pr	2.579	59.8
	O(10)pq	3.194	77.6
O(7)	O(7)t	3.020	78.8
	O(8)s	3.098	79.4
O(7)t	O(8)s	3.643	100.5
	O(10)pq	2.935	78.4
O(8)s	O(9)pr	2.961	76.2
O(9)pr	O(10)pq	3.666	102.4
average		3.210	
Distorted octahedron about Ca(3)pr			
O(4)	O(8)	2.563Å	60.8°
	O(9)pr	3.058	75.7
	O(10)pr	3.064	76.9
O(6)qp	O(7)s	4.196	108.9
	O(8)s	3.680	89.0
	O(9)pr	2.587	59.8
	O(10)pr	3.214	77.8

Table 6. (continued)

Neighbours		Edge length	Angle
O(7)s	O(8)	3.098Å	79.4°
	O(8)s	3.721	100.1
	O(10)pr	2.935	77.3
O(8)	O(8)s	3.176	80.0
O(8)s	O(9)pr	2.961	75.3
O(9)pr	O(10)pr	3.698	104.0
average		3.227	
Tetrahedron about Si(1)			
O(2)	O(4)	2.677Å	112.4°
	O(5)	2.537	100.8
	O(8)	2.648	110.4
O(4)	O(5)	2.717	114.7
	O(8)	2.563	108.4
O(5)	O(8)	2.649	110.1
average		2.632	
Tetrahedron about Si(2)			
O(2)	O(3)	2.691Å	111.6°
	O(6)	2.532	101.1
	O(7)	2.686	110.4
O(3)	O(6)	2.729	113.3
	O(7)	2.652	108.9
O(6)	O(7)	2.713	111.4
average		2.667	
Tetrahedron about Si(3)			
O(1)b	O(5)bc	2.659Å	111.0°
	O(6)c	2.660	111.0
	O(9)	2.603	110.7
O(5)bc	O(6)c	2.634	108.1
	O(9)	2.579	107.8
O(6)c	O(9)	2.587	108.2
average		2.620	
Other distances			
O(10)p	O(10)c	5.128Å	
	O(10)pq	5.965	
	O(10)pr	5.991	

Table 6. (continued)

Neighbours	Edge length	Angle
Bridge angles		
Si(1) −O(2) −Si(2)		142.9°
Si(1)b−O(5)b −Si(3)c		138.7
Si(2) −O(6) −Si(3)c		139.0
Si(3)b−O(1) −Si(3)pc		180.0

Estimated errors are ±0.004Å for Ca-O and Si-O, ±0.005Å for O-O and ±0.2° for angles.
Letters associated to atomic symbols are code indicators showing coordinates of atoms equivalent by space-group operation to the atoms at *xyz* (Table 3).
Corresponding operations are:
b; translation *b*
c; translation *c*
p; inversion center at 1/2, 1/2, 1/2
q; inversion center at 1/2, 3/4, 3/4
r; inversion center at 1/2, 1/4, 3/4
s; inversion center at 0, 1/4, 3/4
t; inversion center at 0, 3/4, 3/4.
Two code indicators in sequence imply an atom related to the one at *xyz* by successive application of the two symbolized operations.

evidence that the structure could be acentric. Therefore, the angle at O(1) seems to be significant. The bridge bond length of 1.600Å for Si(3)-O(1) is indeed very close to the expected value, ~1.596Å for the angle (see Fig. 6a in Gibbs *et al.*, 1972). In turn, the Si(3)-O(9) bond in the same tetrahedron shows small value of 1.565Å. Note that this particular tetrahedron, Si(3), share, with adjacent tetrahedra, three corners, O(1), O(5) and O(6); O(9) is only one non-bridge oxygen atom in the tetrahedron. Such a tetrahedra, which often occurs in silicates like micas and amphiboles, tends to be, in general, elongated towards nonbridge oxygen atoms (Takéuchi, 1975). Contrary to this, the tetrahedron, now considering, is rather flattened. This is explainable because two edges, O(5)-O(9) and O(6)-O(9) which

meet at O(9), are shared with those of the polyhedra about Ca(3) and Ca(2) respectively (Fig. 9); the short bond length for Si(3)-O(9) would probably be, at least in part, due to such a structural hindrance.

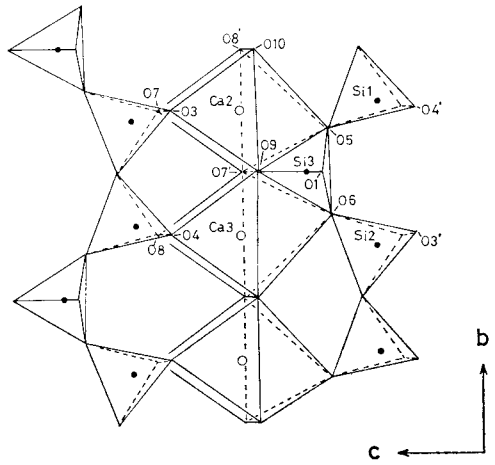

Fig. 9. The linkage of the polyhedra about Ca(2) and Ca(3) and a silicate chain. Small solid and open circles respectively represent Si and Ca atoms.

The tetrahedra about Si(1) and Si(2) also show modes of distortions which are not common in silicates. The *nb* edges are significantly longer than *bb* and *nn* edges; here, *nb*=edge between nonbridge and bridge oxygen atoms. In general, *nb* edges have lengths between those of *nn* and *bb*, or they tend to be smaller than both *bb* and *nn* (Takéuchi *et al.*, 1974). Such an unusual feature of distortion may, in part, be due to the fact that the *nn* edges of the tetrahedra are shared by those of Ca-polyhedra; the *nn* edges are shortened to seal the electrostatic repulsion between Si and Ca. And, in part, to the short O(2)-O(5) and O(2)-O(6) edges (Table 6) respectively for Si(1) and Si(2) tetrahedra. The short edges seem to be due to, like Si(2) tetrahedron in axinite (Takéuchi *et al.*, 1974), the distortion

of tetrahedra arisen from packing the link of both tetrahedra in the restricted space of the structure. In the case of axinite, an edge like this shows an even smaller value of 2.430(2)Å.

Hydrogen locations and polytypism

As observed in Table 5 which gives the estimated bond valences calculated with the method of Donnay and Allmann (1970), the protons occur at O(10) in the form of OH. The atom related to OH by a translation, $\boldsymbol{b}/2$, is O(9) of the Si(3) tetrahedron; this oxygen atom is evidently not equivalent to the hydroxyl group. Therefore when we note the location of hydrogen atoms in the sheet, the pseudotranslation of $\boldsymbol{b}/2$ in the sheet is chemically suppressed. The existence of OH groups in xonotlite has been revealed by infrared spectroscopy (Kalousek and Roy, 1957; Basenow *et al.*, 1964; Rsykin *et al.*, 1969). On the other hand, based on H-NMR spectra, Grimmer and Wieker (1971) suggested that part of protons in their synthetic material were associated with silicate chains, giving a formula:

$$(CaOH)_{2.0}Ca_{3.6}(H_{0.8}Si_6O_{17})\cdot 0.2H_2O.$$

In this expression of chemical formula, the OH group in the same parentheses of Ca is obviously the one at O(10). The location of protons associated with silicate chains can not be decided from the presently available structural knowledge of xonotlite. The H_2O groups would probably be located around the centers of the eight-membered rings of the chains.

Since every OH does not have its pair OH at the position separated by $b/2$, the relative arrangement of OH with respect to others may vary depending upon types of polytypic variants (Gard, 1966). To see this, we classified the possible polytypes of xonotlite into two categories in terms of the following modes of juxtaposition of *p*-xonotlite cells, with (001) as boundary plane:

(1) Parallel and continuous position in the direction of c. The $P2/a$ polytype given by Mamedov and Belov (1955) falls, as mentioned before, in this category (Fig. 8a).

(2) Every other, instead of every, cell is in parallel and continuous position; at the boundary, adjacent cells are displaced relative to each other by $b/2$. The present $A\bar{1}$ structure belongs to this category (Fig. 8b).

A calculation based on the atomic coordinates derived from the present structure shows that in the structures of the first category every OH will have two near neighbours of OH at the distances of 4.710Å and 5.128Å. While, in the structures of the second category, it will have three near neighbours at the distances of 5.128Å, 5.965Å and 5.991Å. The average OH-OH distances are 4.92Å for the former case and 5.70Å for the latter. Grimmer and Wieker (1971) reported based on NMR study on powdered specimens, that the average OH-OH distance in the material was 4.5Å. Base on the above consideration we may predict that their material would have a structure which belongs to the first category.

The authors wish to thank Dr. A. Kato, National Science Museum, Tokyo, for specimens, and Prof. H. F. W. Taylor, University of Aberdeen, for useful comment.

The computations were performed on HITAC 8700/8800 at the Computer Center of the University of Tokyo.

References

Basénow, N. M., Kol'cov, A. I., Kirpičnikova, N. I., Ryskin, Ja. I., Stavickaja, G. P., Boikova, A. I. & Toropov, N. A. (1964) *Izvest. Akad. Nauk SSSR, Ser. Chim.*, **3**, 409-416.

Coppens, P. & Hamilton, W. C. (1970) *Acta Cryst.*, **A26**, 71-83.

Dent, L. S. & Taylor, H. F. W. (1956) *Acta Cryst.*, **9**, 1002-1004.

Donnay, G. & Allmann, R. (1970) *Amer. Miner.*, **55**, 1003-1015.

Evans, H. T. Jr., Appleman, D. E. & Handwerker, D. S. (1963) *Amer. Cryst.*

Assoc. Meeting Cambridge, Program and Abstract, 42.

GARD, J. A. (1966) *Nature*, **211**, 1078-1079.

GIBBS, G. V., HAMIL, M. M., LOUISNATHAN, S. J., BARTELL, L. S. & YOW, H. (1972) *Amer. Miner.*, **57**, 1578-1613.

GRIMMER, A. R. & WIEKER, W. (1971) *Zeits. anorg. allg. Chem.*, **384**, 34-42.

HELLER, L. (1952) *Third International Symposium on the Chemistry of Cement*, 237. Cement and Concrete Association, London.

International tables for X-ray crystallography (1962) III. Kynoch Press, Birmingham.

ITO, T. (1950) *X-ray studies on polymorphism*. Maruzen, Tokyo.

ITO, T., SADANAGA, R., TAKÉUCHI, Y. & TOKONAMI, M. (1969) *Proc. Japan Acad.*, **45**, 913-918.

JOHNSON, C. K. (1965) *ORTEP. Report ORNL-3794*. Oak Ridge National Laboratory, Tennessee.

KALOUSEK, G. L. & ROY, R. (1957) *Journ. Amer. Chem. Soc.*, **40**, 236-239.

KALOUSEK, G. L., MITSUDA, T. & TAYLOR, H. F. W. (1977) *Cement Concrete Res.*, **7**, 305-312.

MAMEDOV, Kh. S. & BELOV, N. V. (1955) *Dokl. Acad. Nauk SSSR*, **107**, 615-618.

MAMEDOV, Kh. S. & BELOV, N. V. (1956) *Zapiskii Vsesoyuz. Miner. Obshchest*, **85**, 13-38.

PREWITT, C. T. & BUERGER, M. J. (1963) *Miner. Soc. Amer. Spec. Paper* **1**, 293-302.

RSYKIN, Ja. I., STAVICKAJA, G. P. & MITROPOL'SKIJ, N. A. (1969) *Izvest. Akad. Nauk. SSSR, neorg. Mat.*, **5**, 577.

TAKÉUCHI, Y., OZAWA, T., ITO, T., ARAKI, T., ZOLTAI, T. & FINNEY, J. J. (1974) *Zeits. Kristal.*, **140**, 289-312.

TAKÉUCHI, Y. (1975) *Contributions to Clay Mineralogy, Sudo Vol.*, 1-6.

TIBA, T. (1974) Cited from KATO, A. & MATSUBARA, S. (1974) *Intern. Miner. Assoc. Ninth General Meeting, Berlin-Regensburg, Abstract*, 96.

YAMANAKA, T., SADANAGA, R. & TAKÉUCHI, Y. (1977) *Amer. Miner.*, **62**, 1216-1224.

Received October 28, 1978.